Mesh Refinement Strategies for Solving Singularly Perturbed Reaction-Diffusion Problems

W. CASTAINGS*
Chambre C503 Residence la Haute Malgrange
Rue Jean Lamour
54500 Vandoeuvre-Les-Nancy, France
wcastaings@yahoo.fr

I. M. NAVON†
Department of Mathematics
Supercomputer Computations Research Institute
Florida State University
Tallahassee, FL 32306-4052, U.S.A.
navon@scri.fsu.edu

Abstract—We consider the numerical approximation of a singularly perturbed reaction-diffusion problem over a square. Two different approaches are compared namely: adaptive isotropic mesh refinement and anisotropic mesh refinement. Thus, we compare the h-refinement and the Shishkin mesh approaches numerically with PLTMG software [1]. It is shown how isotropic elements lead to over-refinement and how anisotropic mesh refinement is much more efficient in thin boundary layers. © 2001 Elsevier Science Ltd. All rights reserved.

Keywords—Singularly perturbed reaction-diffusion, Mesh refinement, Shishkin mesh, PLTMG software.

1. INTRODUCTION

The numerical solution of singularly perturbed boundary value problems has recently received much attention. In fact, problems of this type arise in many areas, such as fluid mechanics and heat transfer, as well as problems in structural mechanics posed over thin domains.

The solution of a singularly perturbed elliptic problem will, in general, contain *shape boundary layers* along the boundary of the domain. If, in addition, the domain contains corners, then the solution will also include singularities in the neighborhood of each vertex.

The coupling of boundary layers and corner singularities may complicate the numerical approximation, and the numerical method must be chosen carefully tailored to account for their presence.

In what follows, we will consider the following singularly perturbed elliptic problem:

$$-\nabla \left(\varepsilon^2 \nabla u\right) + \sigma u = f, \qquad \text{in } \Omega \subset \mathcal{R}^2, \tag{1}$$

$$u = 0, \qquad \text{on } \partial\Omega, \tag{2}$$

where $0 < \varepsilon \ll 1$, σ is a constant, and $f(x, y)$ is analytic. Its weak formulation is: find $u \in H_0^1(\Omega)$ such that

$$a(u, v) := \varepsilon^2 (\nabla u, \nabla v) + \sigma(u, v) = (f, v), \qquad \forall v \in H_0^1(\Omega), \tag{3}$$

where $(., .)$ denotes the usual L^2 inner product.

The Lax Milgram Lemma ensures that there exists a unique solution of (3) provided that

- $f \in [H_0^1(\Omega)]^* = H^{-1}(\Omega)$,
- $a(., .)$ is elliptic, i.e., $a(v, v) \geq \mu_1 . \|v\|_{H_0^1(\Omega)}$, $\forall v \in H_0^1(\Omega)$,
- $a(., .)$ is bounded, i.e., $|a(v, w)| \leq \mu_2 . \|v\|_{H_0^1(\Omega)} . \|w\|_{H_0^1(\Omega)}$, $\forall v, w \in H_0^1(\Omega)$.

In addition, we require a stronger smoothness of the right-hand side, namely that

$$f \in L_2(\Omega)$$

to ensure that the first assumptions is satisfied. The second and third assumption are automatically valid with constants $\mu_1 = \varepsilon^2$ and $\mu_2 = \sigma$.

The finite element approximation of (1),(2) proceeds as usual: given a subspace $V_N \in H_0^1(\Omega)$ of dimension N, the finite element solution $u_N \in V_N$ satisfies

$$a(u_N, v) = (f, v), \qquad \forall v \in V_N. \tag{4}$$

The model problem (1),(2) is of interest since one can usually expect boundary layers when a nonvanishing right-hand side f satisfies homogeneous Dirichlet boundary conditions. In fact, let us consider the limit equation

$$\sigma u_0(x) = f(x), \qquad x \in \bar{\Omega}. \tag{5}$$

One can see that the solution u_0 of the previous equation cannot satisfy the boundary condition (2) and/or is possibly nonsmooth.

Inside Ω and sufficiently far away from the boundary the solution is usually smooth provided f is smooth enough too. Thus, the boundary layers mark the domain of interest, and their resolution requires an increased numerical effort. In [2], it was shown (for smooth domains) that if f is smooth then the difficulty in approximating u lies entirely within the boundary term. In addition, it was shown that the boundary layer effect is essentially one-dimensional, namely in a direction normal to the boundary.

Let h_T be the diameter of the finite element T and ρ_T the largest inscribed ball in T. We will see how the mesh generation routines of PLTMG software package (piecewise linear finite element multigrid developed by Bank and collaborators) [1] allow us to construct either:

- isotropic meshes, meaning that $h_T/\rho_T = \mathcal{O}(1)$ for $\varepsilon \to 0$ and $h \to 0$,
- or anisotropic meshes, implying that $h_T/\rho_T = \infty$ for $\varepsilon \to 0$ and $h \to 0$.

Our goal in this paper is to carry out a numerical comparison between the approaches exposed previously discussed. First, in order to illustrate the properties of the solution and also to justify the use of mesh refinement strategies, computations will be carried out on a uniform mesh. Then we will experiment with adaptive h-refinement (isotropic mesh refinement) in Section 2, and with a Shishkin mesh (anisotropic mesh refinement) in Section 3. In Section 4, a synthesis of

reaction diffusion

(a) u_h.

reaction diffusion

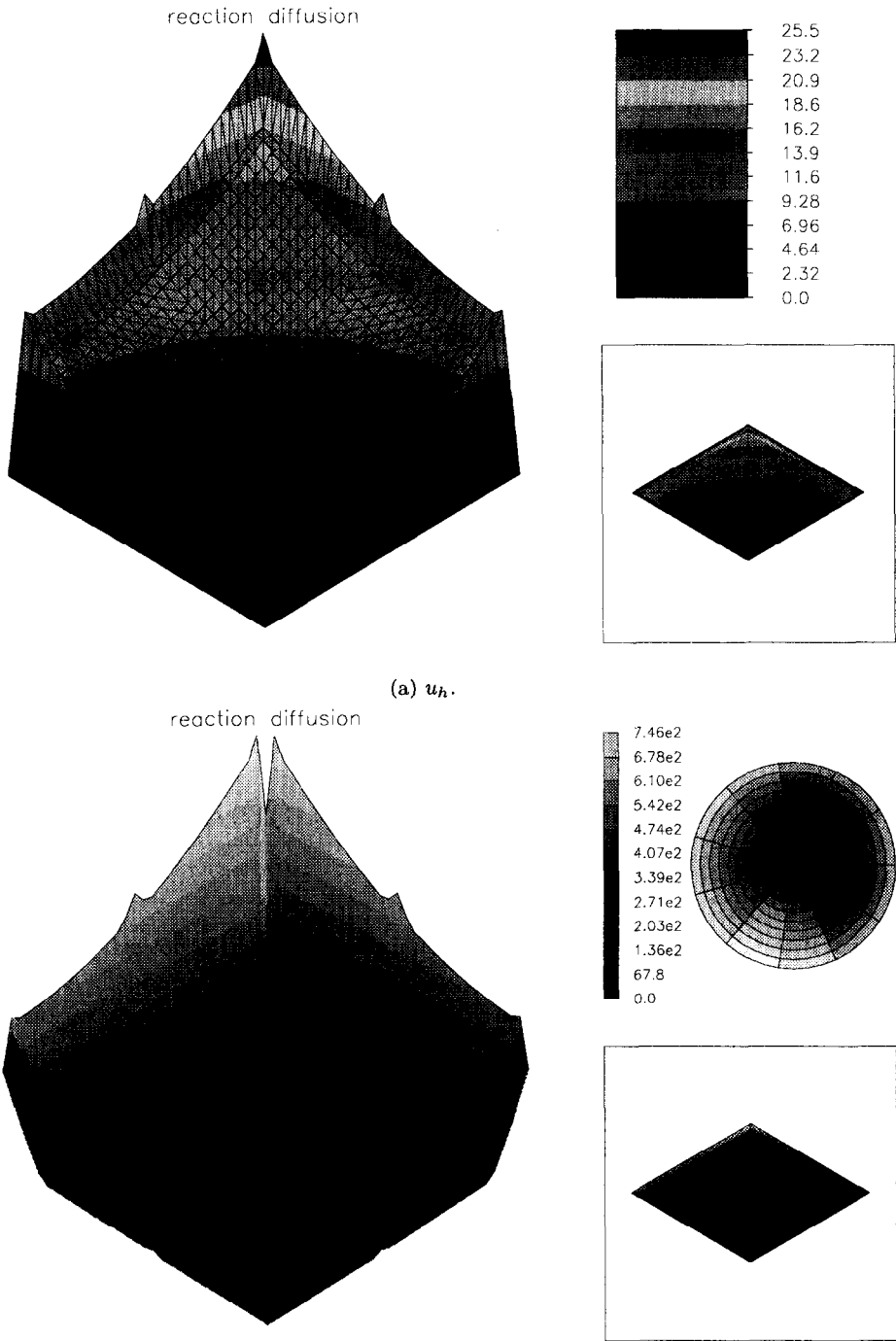(b) ∇u_h ($\varepsilon = 1.0E - 02$).

Figure 1.

the results obtained in the previous sections is carried out. Finally, conclusions are presented in Section 5.

Throughout the paper, numerical implementation will be carried out with the test examples experimented in [3], namely the following examples.

EXAMPLE 1. Where $\sigma = 2$ and $f = 20(x^2 + y^2) + 4$ in (1). In this example, the function f meets the Dirichlet boundary conditions on the four sides of the unit square; the sharper boundary layers are located on sides $x = 1$ and $y = 1$ and a corner layer is observed at $(1,1)$, respectively.

Example 2. Where $\sigma = 2$ and f are such that exact solution is

$$u(x,y) = \left(1 - \frac{e^{-x/\varepsilon} + e^{-(1-x)/\varepsilon}}{1 + e^{-1/\varepsilon}}\right)\left(1 - \frac{e^{-y/\varepsilon} + e^{-(1-y)/\varepsilon}}{1 + e^{-1/\varepsilon}}\right),\tag{6}$$

the exact solution is known and does not have corner singularities; however, exponential boundary layers exist on the four sides of the unit square.

2. PLTMG FEATURES

This software package was developed by Bank and collaborators [1] for solving general elliptic systems of partial differential equations and is available in the public domain.

In order to solve a particular problem, one has to construct an initial mesh or skeleton, generate a mesh from this structure, and solve the equation on the obtained mesh. For adaptive refinement, the mesh generator and equation solver have to be used iteratively.

The software provides a generator of unstructured meshes, moreover h-refinement or unrefinement, r-refinement (moving mesh) are also implemented. In addition, the quality of any adaptive algorithm ultimately rests on the reliability and robustness of the *a posteriori* error control. Thus, one can easily realize the importance of having robust and reliable estimators for singularly perturbed problem. The robustness of the implemented estimator for the singularly perturbed reaction-diffusion equation was shown in [4,5].

The solver deals with boundary value problems using a piecewise linear finite element method, the adaptive mesh refinement, and a multi-level iterative method to solve the resulting sets of linear equations.

As our problem does not invoke continuation, equation (1),(2) can be written as follows:

$$F(u) = 0.\tag{7}$$

In addition, if the Jacobian of the previous optimization problem is not self-adjoint (for convection-diffusion equation for example) some upwinding terms from [6] are added. A damped Newton Method (see [7]) is used to solve problem (7). As part of Newton's Method, various large sparse systems of linear equations have to be solved.

Highly refined meshes will be required in some regions of the domain in order to resolve the boundary layers. Thus, one could assume that the resulting linear system of equations will be ill conditioned, leading to slow convergence of iterative methods and even of direct methods. However, in [8] Bank and Scott prove that the condition number of the linear systems representing the finite element discretization need not degenerate as the mesh is refined locally, provided certain restrictions on the mesh size are met and a natural scaling of the basis functions is used.

The PLTMG package allows the user to process to adaptive refinement based on the interpolation error of a given function. Thus, using these tools will permit us to obtain the interpolation error of the exact solution on a given grid.

In addition, a "global weighted root mean-square norm" (weighted RMS) was implemented in order to carry out a comparison between different methods.

In fact, let u be the exact solution, u_h the computed solution, NVF the current number of vertices; and let e_i be

$$e_i = u(v_i) - u_h(v_i), \qquad i = 1, \text{NVF},\tag{8}$$

the difference between the exact and computed solution at one of the NVF vertices v_i of the triangulation created by PLTMG. Thus, the norm implemented is given by

$$\|u - u_h\| = \left(\frac{1}{\text{NVF}} \cdot \sum_{i=1}^{\text{NVF}} (w_i.e_i)^2\right)^{1/2}.\tag{9}$$

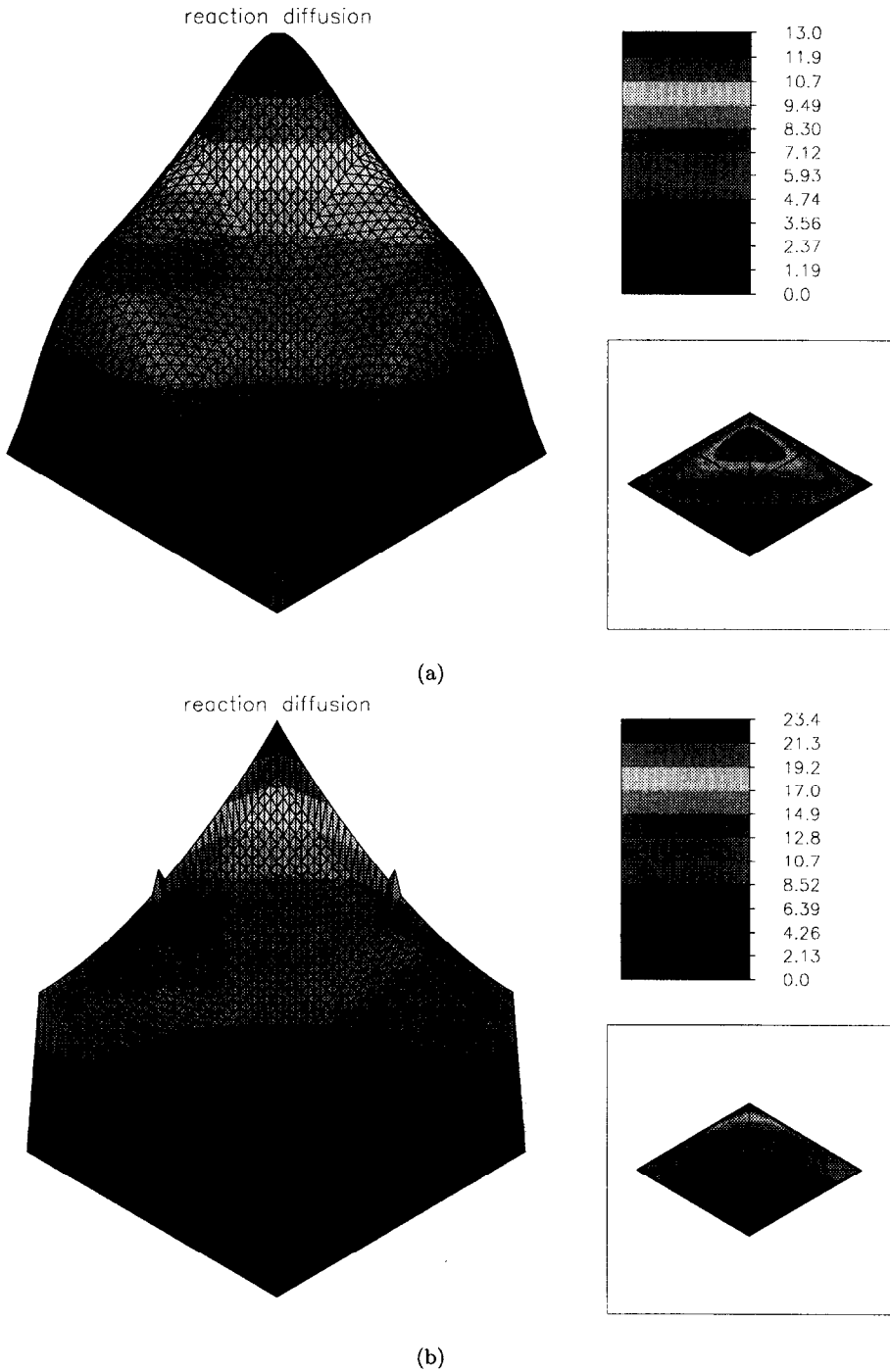reaction diffusion

(a)

reaction diffusion

(b)

Figure 2. Influence of the perturbation parameter on the boundary layers.

Here the weight w_i corresponds to the area of all the triangles which contain the vertex v_i. This combination of weighted and root-min square error allows us to carry out a pertinent comparison between different type of meshes (uniform, nonuniform, isotropic, anisotropic) for several number of vertices.

3. UNIFORM MESH COMPUTATIONS

In this section, we will try to underline the limitations of using a uniform mesh for the solution of singularly perturbed reaction-diffusion equations and also to verify the properties of the solution of our model problem.
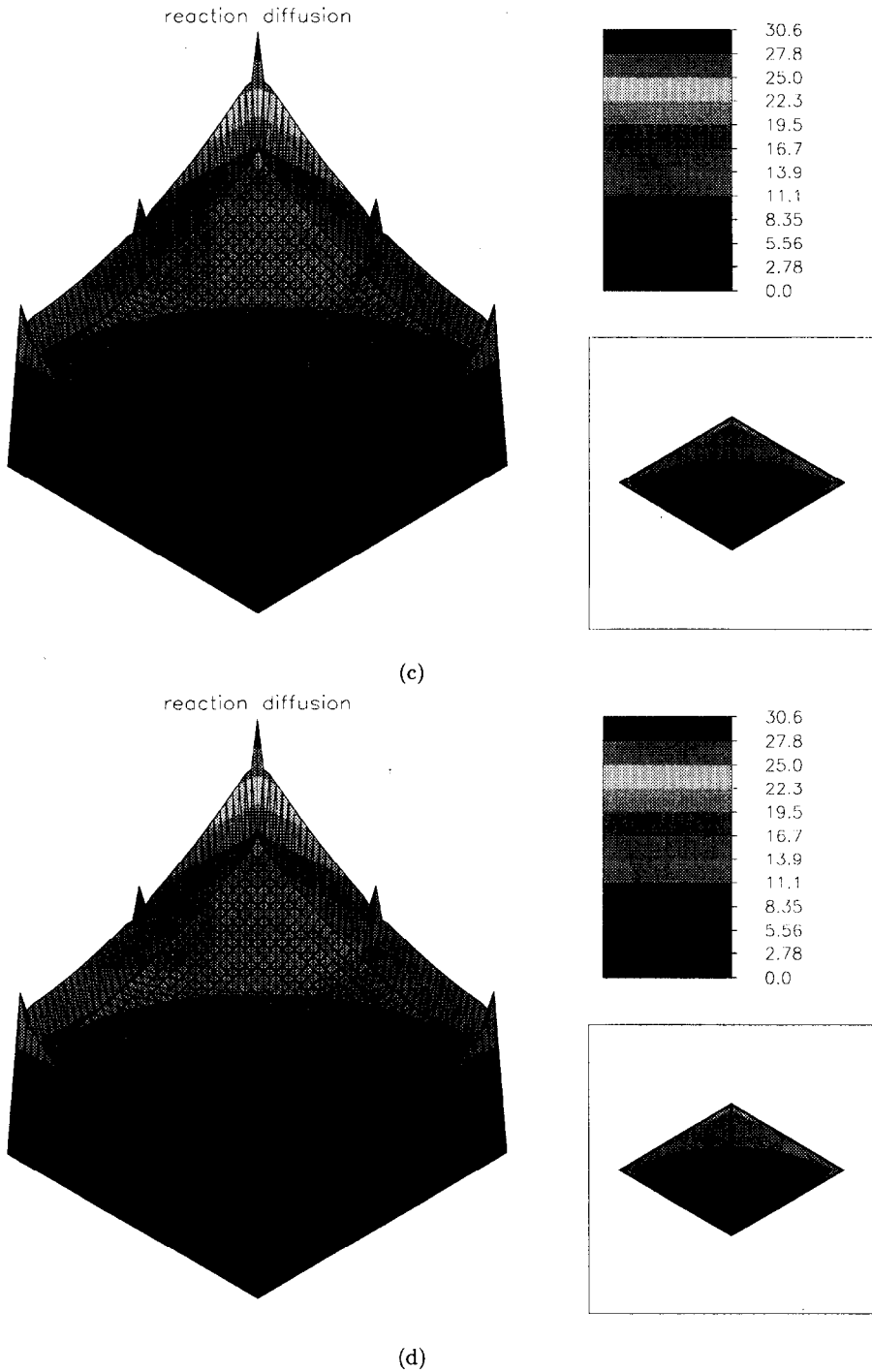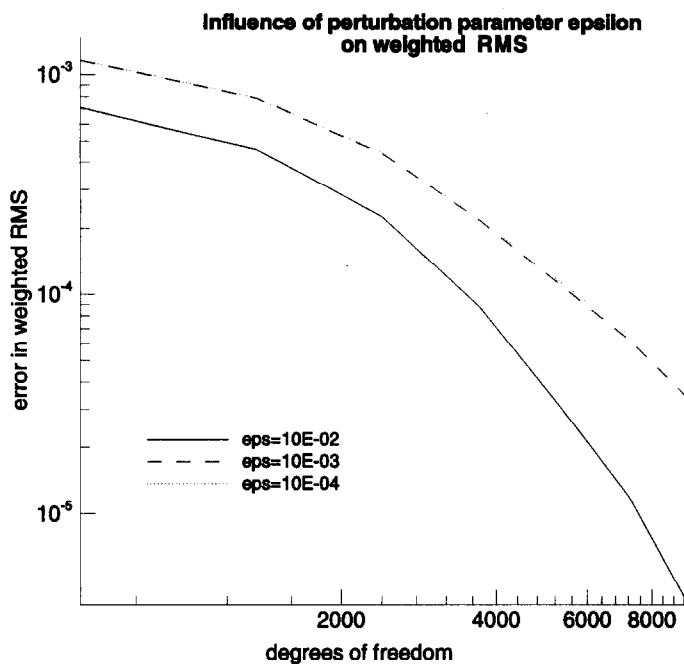
(c)

(d)

Figure 2. (cont.) Influence of the perturbation parameter on the boundary layers.

Previously, Xenophontos has shown in [9] that the solution of our model problem over a nonsmooth domain (square) can be decomposed into a smooth part, a corner layer part and a smooth remainder. In addition, in [10] it was shown that the boundary layer part of the solution is essentially of the form
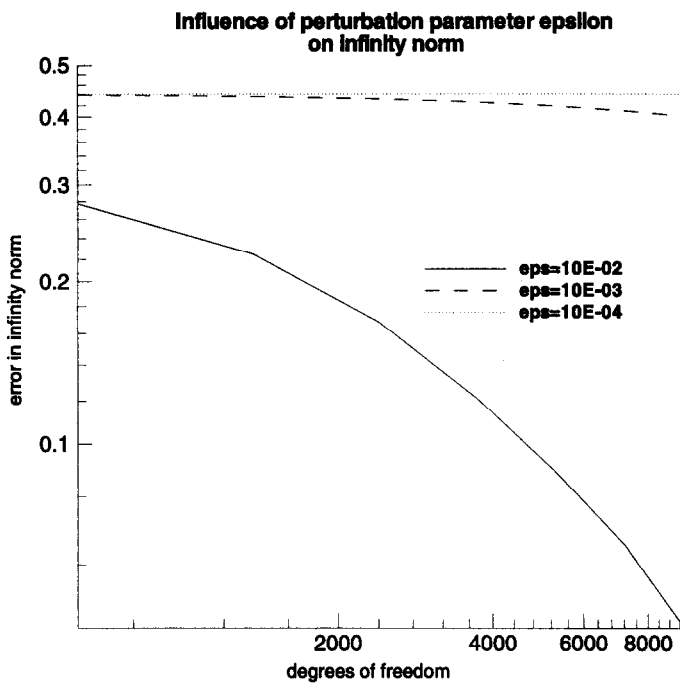
$$u_{BL}(x, y) = C(x) \exp\left(-\frac{y}{\varepsilon}\right) \tag{10}$$

with $C(x)$ smooth. This indicates that the boundary layer effect is essentially one dimensional.

Let us take Test Example 1 and solve the equation on the unit square on a uniform grid. It is obvious from Figure 1a that the sharp boundary layers could not be easily resolved by the

**Influence of perturbation parameter epsilon
on weighted RMS**

(a) "Weighted RMS norm" convergence.

**Influence of perturbation parameter epsilon
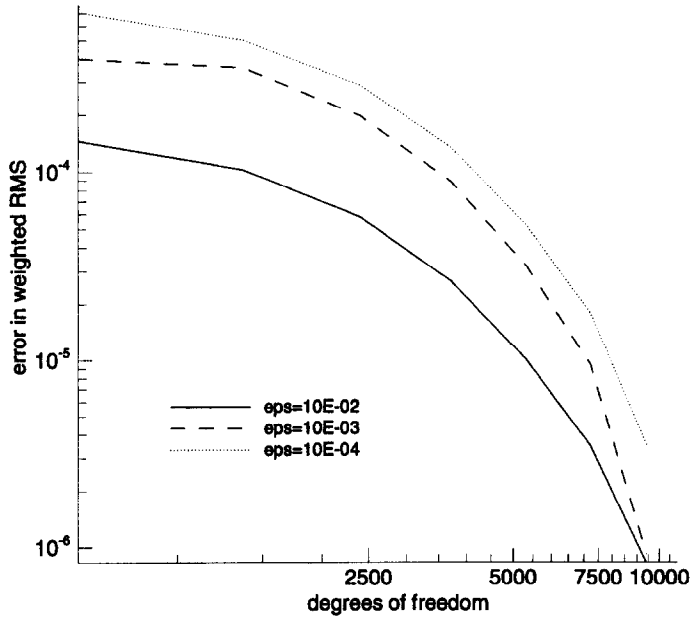on infinity norm**

(b) Infinity norm convergence for $\varepsilon = 10^{-j}$, $j = 2, 3, 4$.

Figure 3.

uniform mesh. In Figure 1b, the different shades of black correspond to different directions in the vector ∇u_h, and different intensities of black correspond to the magnitude of the vector. Thus, one can see that near the boundaries the direction of the gradient vector roughly changes and has higher magnitudes. Moreover, one can see that on each boundary, the direction of the gradient vector is constant. This is an illustration of the typical one-dimensional boundary layer mentioned previously.
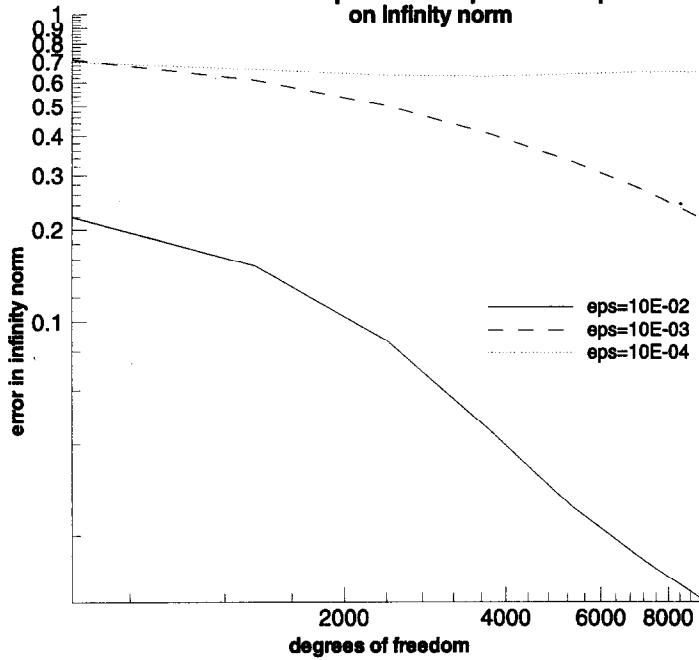
In addition, the perturbation parameter ε has an important influence on the structure of boundary layers. In fact, as $\varepsilon \rightarrow 0$ the boundary layer becomes sharper (for $\varepsilon \leq 10^{-4}$ there is

Influence of perturbation parameter epsilon on weighted RMS norm

(a) "Weighted RMS norm" convergence.

Infulence of perturbation paramater epsilon on infinity norm

(b) Infinity norm convergence for $\varepsilon = 10^{-j}$, $j = 2, 3, 4$.

Figure 4.

no distinction from the case $\varepsilon = 10^{-4}$). Figures 2a–2d were obtained with different values of perturbation parameter ε, namely,

(a) $\varepsilon = 1.0E - 01$,

(b) $\varepsilon = 1.0E - 02$,

(c) $\varepsilon = 1.0E - 03$,

(d) $\varepsilon = 1.0E - 07$.

As shown in [11], global estimates uniformly in ε can be derived in the L_2 norm

$$\|u - u_h\|_{L_2(\Omega)} \le C \min\left(\sqrt{h}, h^2 \varepsilon^{-3/2}\right), \tag{11}$$

so that uniform convergence of order $1/2$ occurs. Moreover, the infinity norm is of interest since one needs to consider the error in the very small domains in which the boundary layers occur. In fact, use of other usual norms, such as the root mean square, involve averages of the error which smooth out rapid changes in the solutions, and therefore, fail to capture the local behavior of the error in these layers. Considering the form of the boundary layer term in (11) and key results from [11], we can guess that for this Dirichlet problem the finite element method on a uniform mesh cannot converge uniformly in ε in the global norm $\| \quad \|_{L_\infty(\Omega)}$. The error in L_∞ as well as "weighted RMS norm" were computed for Test Example 2 (where the exact solution is known).

In Figure 3a, one can notice that the finite element method on uniform meshes converges but when ε decreases, the accuracy of the solution is altered. However, the results displayed in Figure 3b which exhibit uniform convergence in ε cannot be obtained using the standard finite element method on a uniform mesh.

As an alternative approach, we are going to focus on the use of standard finite element methods on highly nonuniform meshes.

4. ISOTROPIC ADAPTIVE MESH REFINEMENT

As a result of using the mesh generations routines of PLTMG software, we can fully implement an adaptive h-refinement. In this adaptive mesh refinement process the quality of the triangulation is optimized. In fact, for a given triangle $\mathcal{T}$ of area a and side length h_1, h_2, and h_3 the quality is measured using the formula

$$q(\mathcal{T}) = 4 \frac{\sqrt{3a}}{(h_1^2 + h_2^2 + h_3^2)}. \tag{12}$$

The function $q(\mathcal{T})$ is normalized to equal one for an equilateral triangle and to approach zero for triangles with small angles. In order to compute a high quality triangulation, the criteria used by PLTMG package is

$$q(T) \ge 0.6. \tag{13}$$

This feature renders the adaptive refinement process isotropic.

We have already emphasized the importance of robust *a posteriori* error estimates for our problem. Thus, in order to provide a numerical illustration of its robustness, adaptive mesh refinement is carried out for an example where knowledge of the exact solution is available and with error estimates. In fact, let e_Π be the interpolation error for the grid obtained by mesh refinement with *a posteriori* error estimates and E_Π the interpolation error resulting for the grid from refinement with knowledge of exact solution. Let d_Π be

$$d_\Pi = \frac{E_\Pi}{e_\Pi}, \tag{14}$$

so that this coefficient is equal to one for grids with the same interpolation error. A similar coefficient could be also computed for the global weighted root mean square error so that

$$d_{wr} = \frac{E_{wr}}{e_{wr}}. \tag{15}$$

Table 1 provides the obtained coefficient for a h-refinement computation carried out with 2401 vertices. One can see that the performance of the *a posteriori* error estimates appears to be independent from the perturbation parameter ε.

initial shishkin mesh
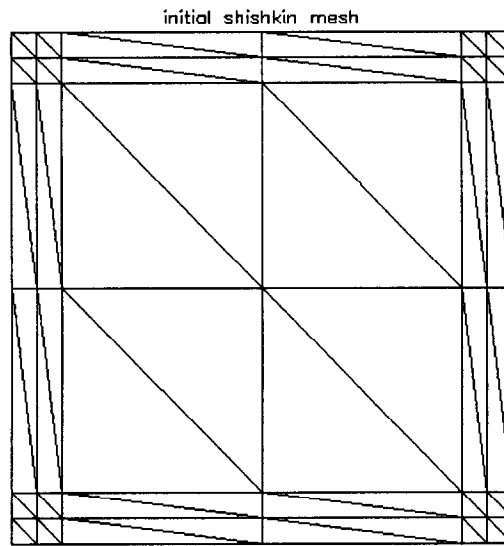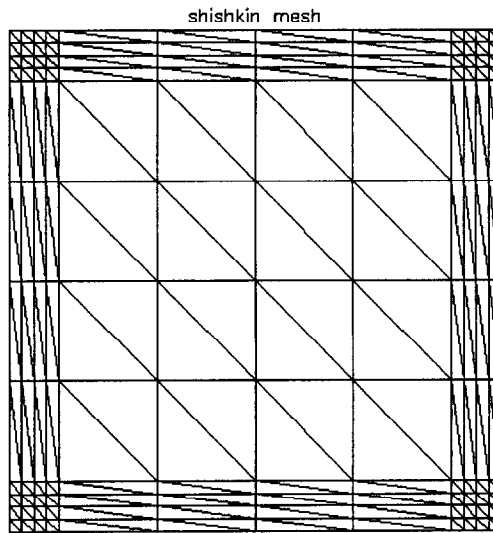

(a) Starting triangulation.

shishkin mesh

(b) Uniform refinement $irefn = 2$.

Figure 5. Shishkin mesh construction.

Table 1. Computed coefficients for $\varepsilon = 10^{-j}$, $j = 2 \ldots 7$.

h-Refinement Computation		
ε	d_Π	d_{wr}
1.0D-02	0.9015	0.9397
1.0D-03	0.9880	0.9317
1.0D-04	1.0914	1.1999
1.0D-05	1.0669	1.0369
1.0D-06	1.0512	0.9894
1.0D-07	1.0873	1.0791

Within the range of values expressed previously, positive constants C_1 and C_2 can be found that are ε-independent such that either of the following inequalities:

$$C_1 e_\Pi \leq |||E_\Pi||| \leq C_2 e_\Pi$$
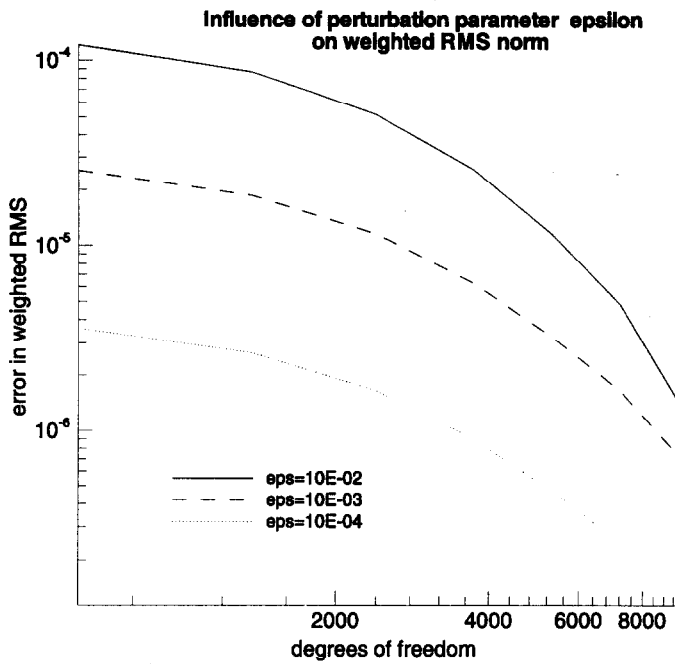
(a) "Weighted RMS norm" convergence.
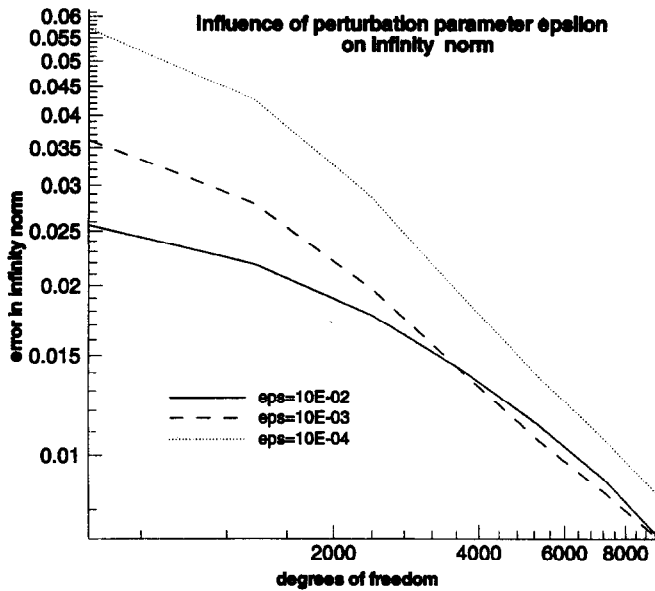
(b) Infinity norm convergence for $\varepsilon = 10^{-j}$, $j = 2, 3, 4$.
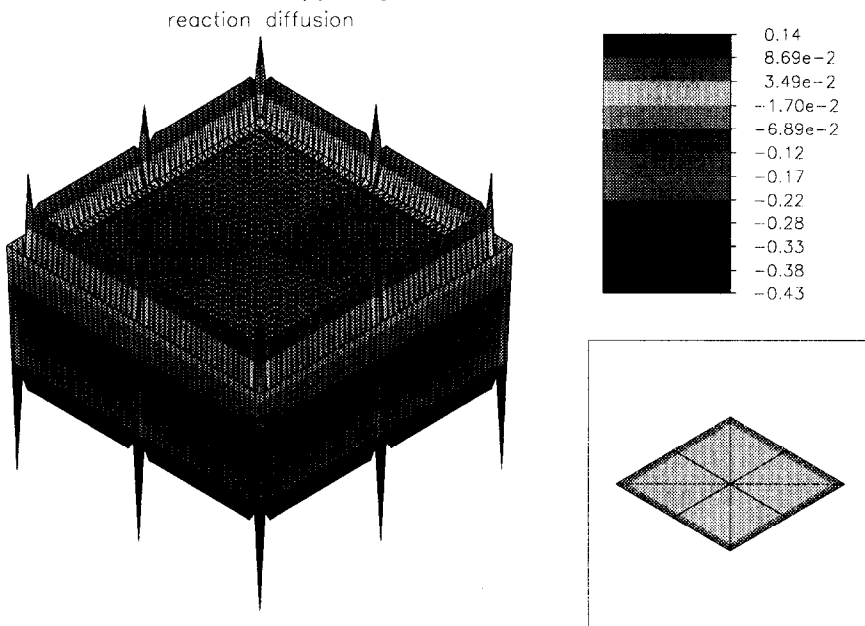
Figure 6.

or

$$C_1 e_{wr} \leq |||E_{wr}||| \leq C_2 e_{wr}$$

holds. Computation with other target values for the number of vertices were also carried out in order to illustrate the h-independence of the estimator. In [9], it was shown that the h-adaptive version of the finite element method (i.e., the degree p of the approximating polynomial being fixed at a low level, here $p = 1$) limits the rate of convergence to an algebraic one. As in the previous section, error in L^∞ as well as the "weighted RMS norm" were computed for Test Example 2. In Figure 4a, the results displayed in Figure 4a show that as for the uniform mesh, nonuniformity in ε is observed when $\varepsilon \geq 10^{-3}$. A nonuniform rate of convergence is obvious by considering Figure 4b.
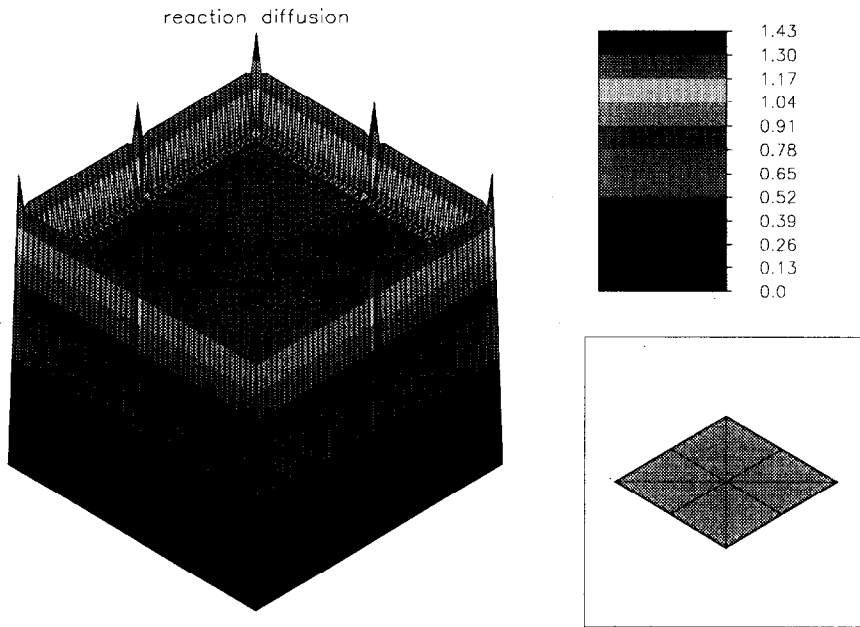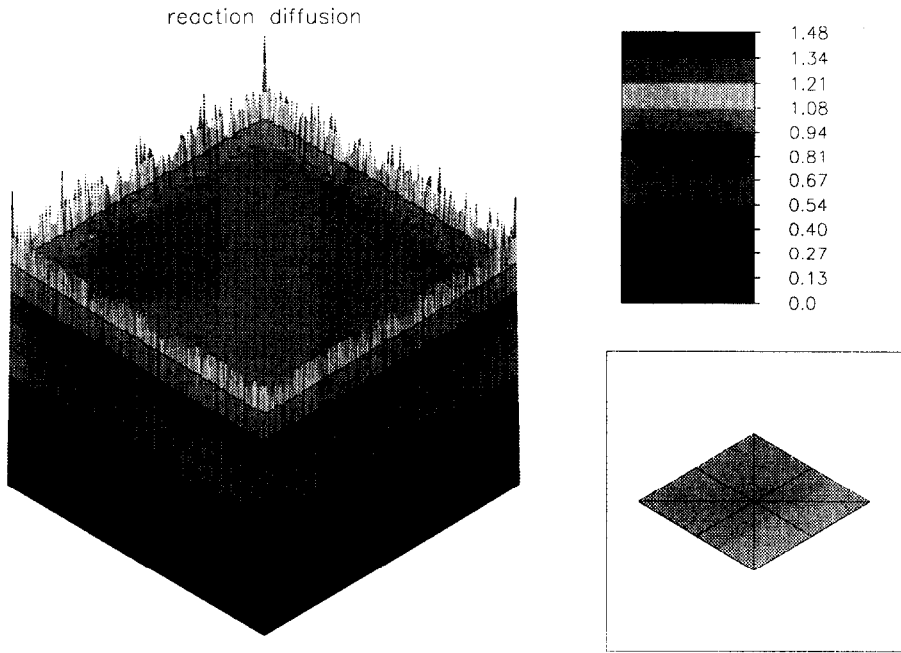
(a) Computed solution.

(b) Pointwise error.

Figure 7. Example 2. Computation on uniform mesh with $N = 2401$ vertices.

As a conclusion, the adaptive h-refinement process is ε-dependant and an accurate solution requires a highly refined mesh near the boundaries.

An alternative way to carry out mesh refinement is to refine the mesh anisotropically based on *a priori* knowledge. This approach will be experimented with for our model problem in the following section.

5. ANISOTROPIC MESH REFINEMENT: SHISHKIN MESH

An *a priori* specified mesh may be either graded [2] or piecewise uniform [3]. Similar to the implementation carried out in [12] for convection-diffusion problems, will experiment with the implementation of piecewise uniform meshes with the PLTMG package.

reaction diffusion

(a) Computed solution.

reaction diffusion
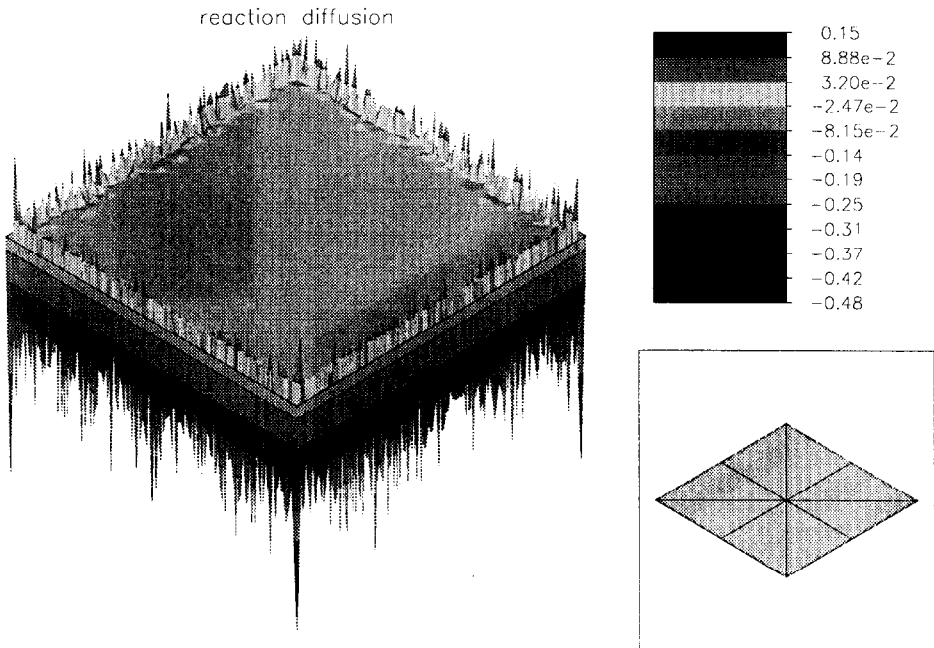
(b) Pointless error.

Figure 8. Example 2. Computation adaptively refined mesh with $N = 2401$ vertices.

The solutions of model problem (1),(2) are characterized by the presence of a boundary layer of width $\mathcal{O}(\varepsilon \ln(1/\varepsilon))$ (see [13]). Shishkin [14] introduced a piecewise uniform mesh (no attempt to change the mesh smoothly) that is designed to yield convergence inside boundary layers. Thus, the resulting meshes are isotropic away from the boundary layers as well as in the corners and anisopically refined close to the boundary manifold.

The Shishkin mesh generation does not require a sizable coding effort due to the uniform mesh refinement routine provided within PLTMG package. In fact, one has to specify the initial mesh filling the triangulation data structures, then the uniform mesh refinement controlled by

reaction diffusion

(a) Computed solution.

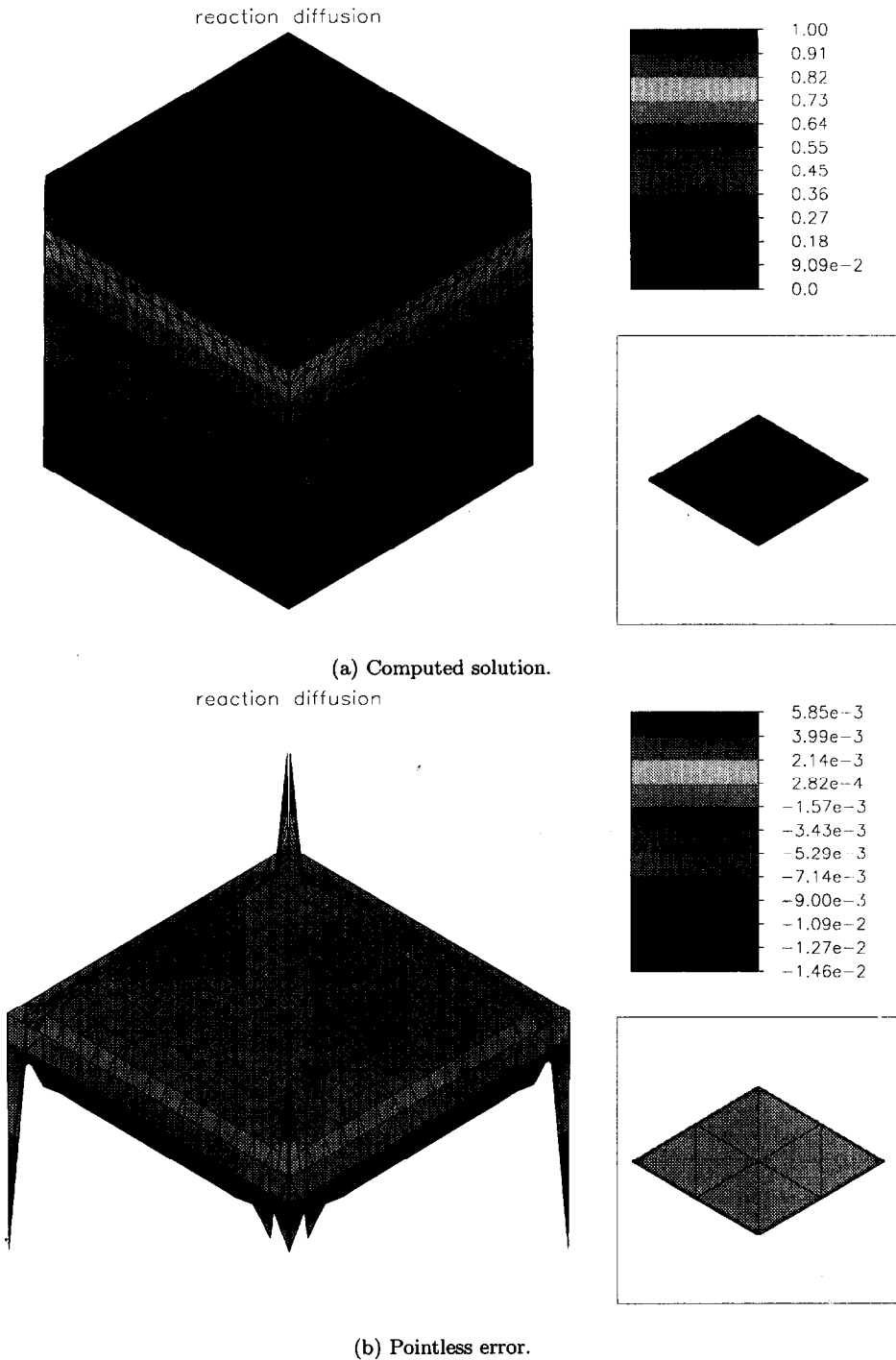reaction diffusion

(b) Pointless error.

Figure 9. Example 2. Computation Shishkin mesh with $N = 2401$ vertices.

parameter $irefn$ (each triangle is divided in $irefn^2$ subtriangles) will generate the desired mesh preserving the geometry imposed by the starting grid.
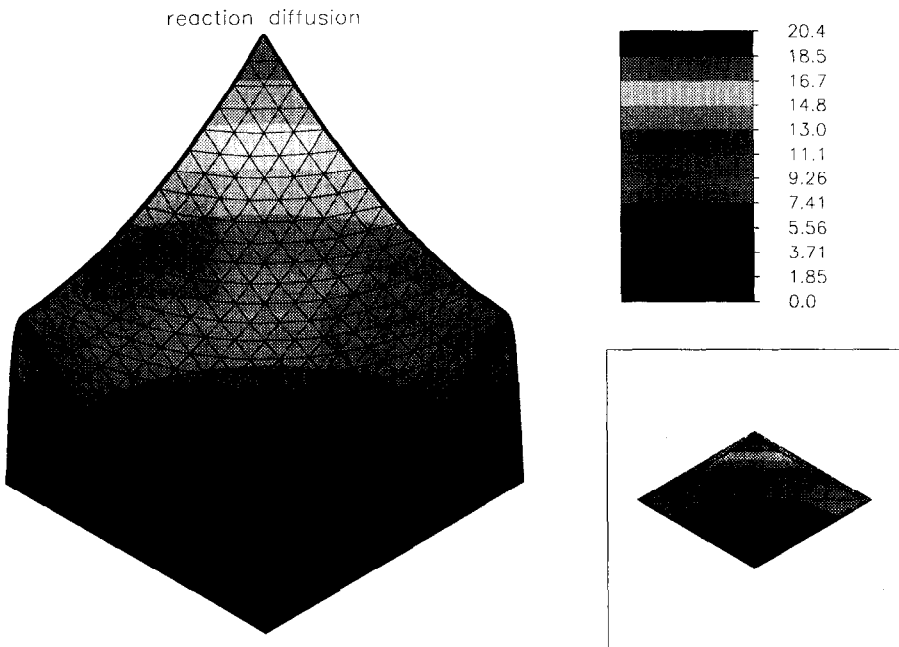
The process for Shishkin mesh type generation with PLTMG package is illustrated in Figure 5 were the thickness of the layer is intentionally kept to be of important size (in order to allow an easily visible process).

Let the thickness of the boundary subdomains be

$$\lambda = C\varepsilon \ln \frac{1}{\varepsilon}, \qquad (16)$$

reaction diffusion

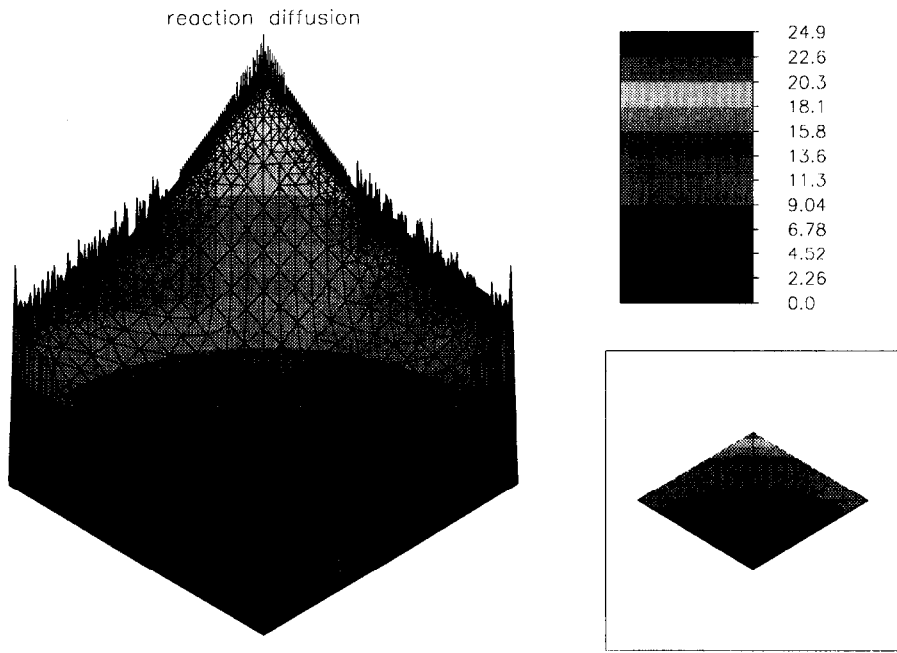
(a) Adaptive mesh refinement.

reaction diffusion
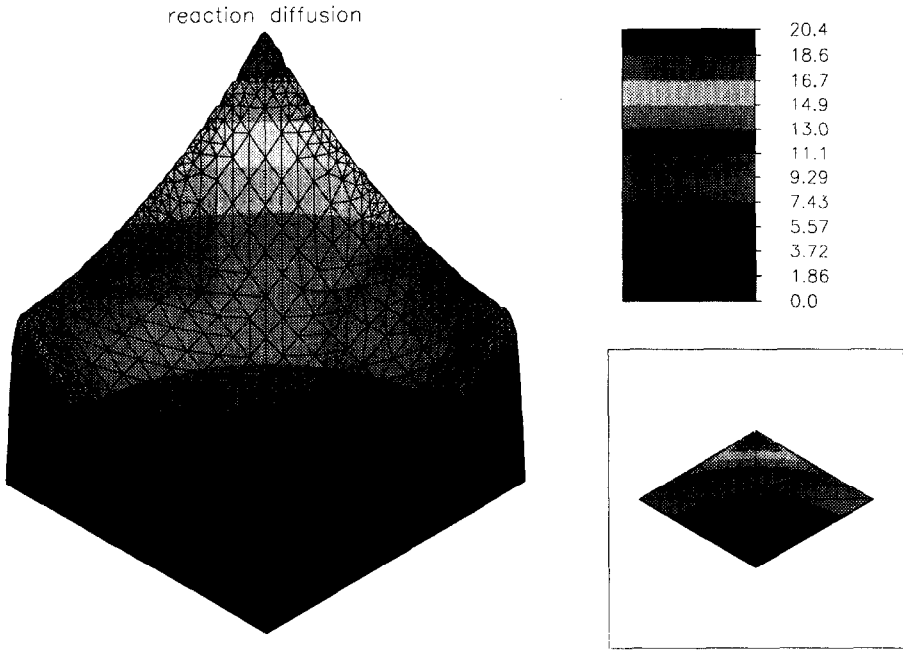
(b) Shishkin mesh.

Figure 10. Example 2. Computation with $\varepsilon = 10^{-2}$ ($N = 2401$ vertices).

where C is a scalar. First, in order to investigate the influence of anisotropic mesh refinement on the approximation, we varied the thickness of the boundary subdomains (where the anisotropic refinement takes place) and computed the solution for an increasing number for degrees of freedom and for a variable perturbation parameter ε. Computed results are provided in Tables 2–4.

One can see that in agreement with results obtained by Apel and Lube for another test example (see [13]) that if C is chosen too large or too small then the interpolation error increases. It was conjectured from this test that an optimal C is dependent on ε in a nonlinear manner. In addition, Figure 6a allows us to validate one of the most important theoretical statement of [13] the one

reaction diffusion

(a) Adaptive mesh refinement.

reaction diffusion
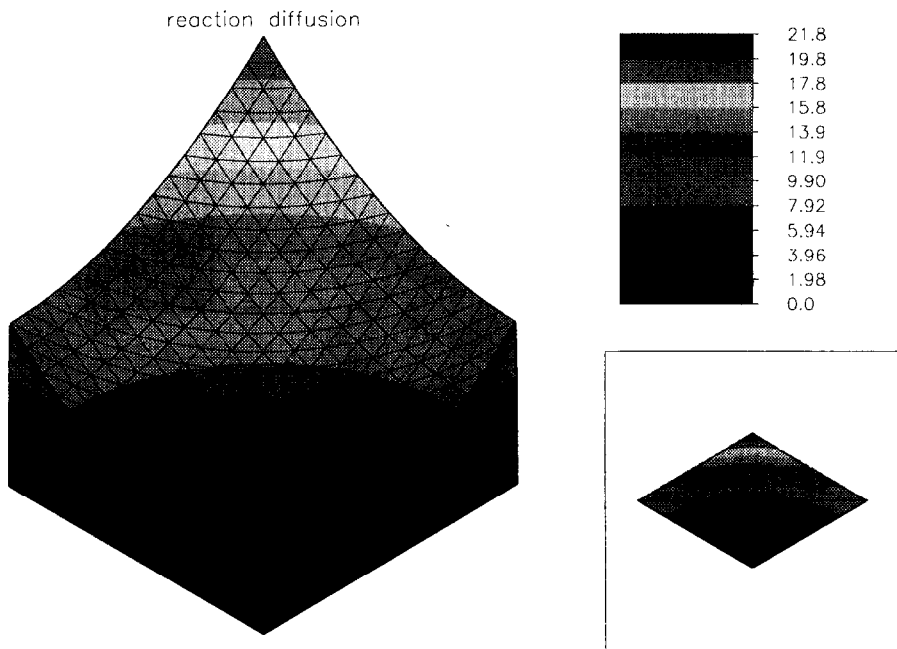
(b) Shishkin mesh.

Figure 11. Example 2. Computation with $\varepsilon = 10^{-3}$ ($N = 2401$ vertices).

asserting that the L_2 error is diminishing with decreasing ε (see Table 5) even in the infinity norm (see Figure 6b).

6. NUMERICAL COMPARISON OF THE DIFFERENT STRATEGIES

It is obvious that the three methods described and experimented with in the previous sections do not posses an identical behavior when applied to our singularly perturbed reaction-diffusion model.

Table 2. Computation for $C = 1$.

Interpolation Error in L^2 Norm for $C = 1$			
N	$\varepsilon = 10^{-2}$	$\varepsilon = 10^{-3}$	$\varepsilon = 10^{-5}$
625	3.6301D−02	1.3986D−02	1.9169D−03
2401	2.2446D−02	9.4750D−03	1.2925D−03
5329	1.4992D−02	7.6218D−03	1.0384D−03

Table 3. Computation for $C = 2$.

Interpolation Error in L^2 Norm for $C = 2$			
N	$\varepsilon = 10^{-2}$	$\varepsilon = 10^{-3}$	$\varepsilon = 10^{-5}$
625	5.8763D−03	2.3321D−03	5.8221D−04
2401	3.0723D−03	7.4200D−04	1.5593D−04
5329	1.9789D−03	4.5783D−04	7.0470D−05

Table 4. Computation for $C = 3$.

Interpolation Error in L^2 Norm for $C = 3$			
N	$\varepsilon = 10^{-2}$	$\varepsilon = 10^{-3}$	$\varepsilon = 10^{-5}$
625	7.0160D−03	4.7902D−03	4.7902D−03
2401	1.8368D−03	1.2662D−03	1.2662D−03
5329	8.4097D−04	5.6912D−04	5.6912D−04

Table 5. Complete results for $C = 2$.

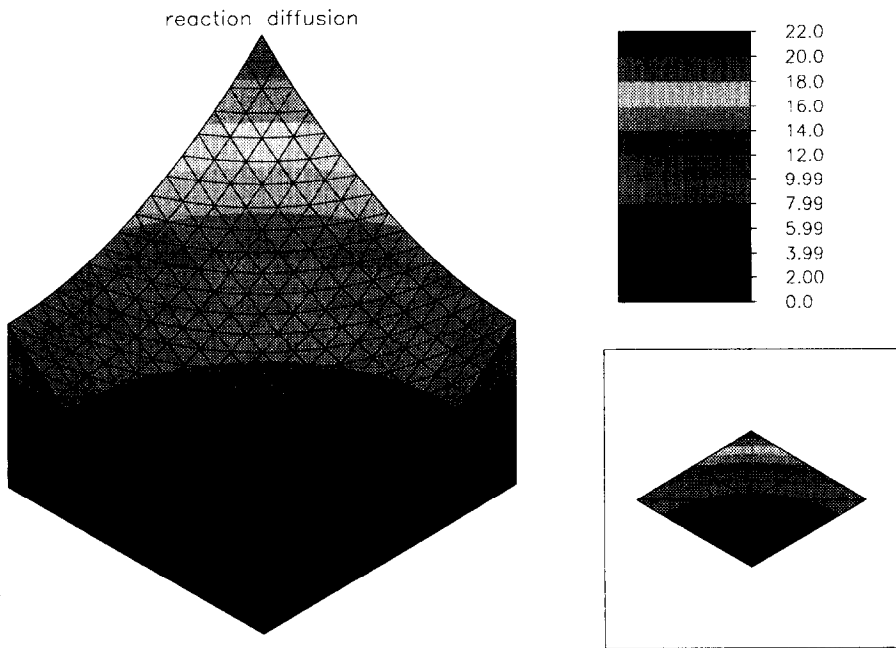| Shishkin Mesh Computation with $C = 2$ $\|u - \Pi_h(u)\|_{L_2(\Omega)}$			
$\varepsilon \backslash N$	625	2401	5329
1.0D−02	5.87630693D−03	3.07237814D−03	1.97890281D−03
1.0D−03	2.33211103D−03	7.42005810D−04	4.57839801D−04
1.0D−04	1.21986926D−03	3.24387770D−04	1.51636927D−04
1.0D−05	5.82216718D−04	1.55938954D−04	7.04701725D−05
1.0D−06	2.55452412D−04	7.01785449D−05	3.17941372D−05
1.0D−07	1.05492244D−04	2.98420605D−05	1.36042865D−05

In this section, numerical experiments are carried out for both of the test examples studied by Li and Navon (see [3]) in order to carry out a comparison between the previously discussed methods.

First, let us compute the solution for a number of 2401 vertices and for a perturbation parameter of $\varepsilon = 10^{-4}$. In Figures 7–9, one can see that the Shishkin mesh approach is by far superior to the other approaches. In fact, the boundary layers are not resolved (for this target value of 2401 vertices) by either the uniform mesh or by the adaptively refined mesh. The pointwise error graphics ((b) for each figure) permit us to provide a numerical illustration of the efficiency of anisotropic meshes in the manifolds where the layers are located. In fact one can see that the error is much larger on the boundaries with the uniform and adaptively refined mesh but also in the corners of the Shishkin meshes. All the previously mentioned areas correspond to subdomains of the mesh where the finite elements are isotropic.

We confirmed previously that the adaptive mesh refinement method does not converge uniformly in ε for the infinity norm while the Shishkin approach converges in this norm. Figures 10–12 show how the accuracy of the solution is altered when $\varepsilon \to 0$ and how the Shishkin mesh performs satisfactory even in the limit case.

reaction diffusion

(a) Adaptive mesh refinement.

reaction diffusion
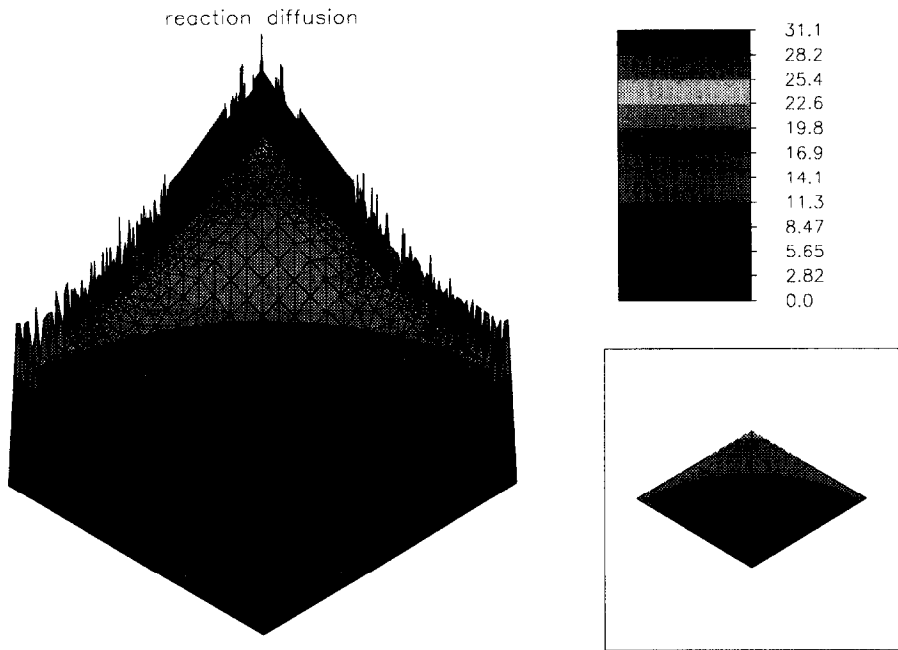
(b) Shishkin mesh.

Figure 12. Example 2. Computation with $\varepsilon = 10^{-4}$ ($N = 2401$ vertices).

Last, the results obtained for each of the approaches were plotted together (see Figure 13 a–c). For larger values of the perturbation parameter, the Shishkin mesh does not yield better results (in the weighted RMS norm) than the adaptively refined mesh (cf., Figure 6a). However, one can notice that as ε decreases, Shishkin method becomes the more efficient.

7. CONCLUSIONS

In this paper, numerical experiments were carried out aiming at comparing results obtained for solving singularly perturbed reaction-diffusion equations for both adaptively refined mesh and
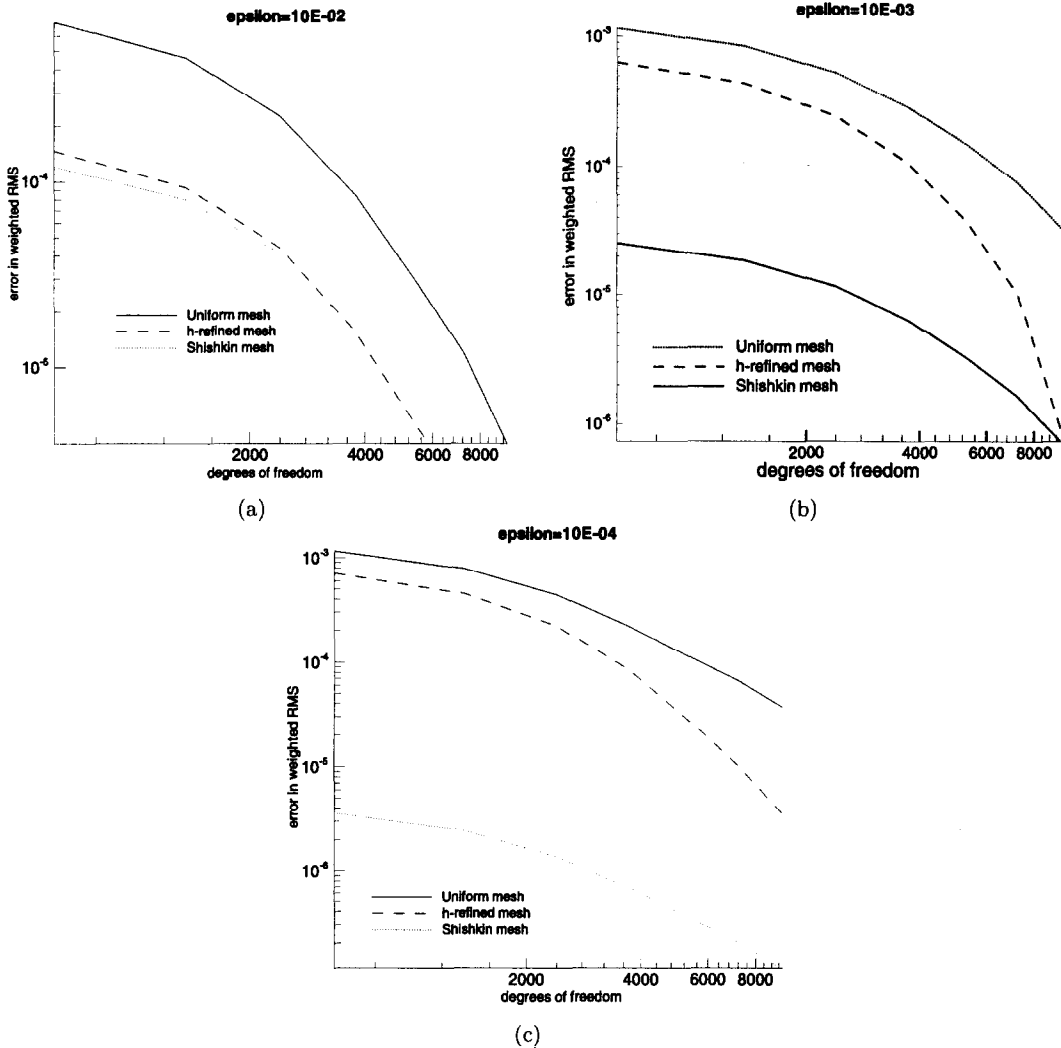
Figure 13. Comparison of strategies for $\varepsilon = 10^{-j}$, $j = 2, 3, 4$.

special anisotropic mesh of Shishkin type. The results obtained in [12] for convection-diffusion problems were extended to reaction-diffusion problems while those obtained by Apel and Lube (see [13]) were confirmed.

For a comparable number of nodes, the Shishkin type meshes yield much better results and do not degrade for limit values of the perturbation parameter. The efficiency of anisotropic finite elements for boundary layers was emphasized. In order to deal with problems with interior layers (straight or curved) similar to those treated by Madden and Stynes in [12] or with general problems without *a priori* knowledge available, it would be interesting to apply error estimates in conjunction with anisotropic meshes. Thus, anisotropic interpolation estimates and anisotropic residual error estimator could be implemented with PLTMG package.

In addition, implementation of piecewise uniform meshes with a nonuniform order of approximation as well as full hp-adaptively refined meshes is also an area where further research should be conducted.

REFERENCES

1. R.E. Bank, *PLTMG: A Software Package for Solving Elliptic Partial Differential Equations Users Guide 8.0*, Philadelphia, PA, (1998).
2. C.A. Xenophontos, Optimal mesh design for the finite element approximation of reaction-diffusion problems, Technical Report TR99-01, Department of Mathematics and Computer Science, Clarkson University, (1999); http://www.clarkson.edu/~christos/PSFILES/publications.html.

3. J. Li and I.M. Navon, Uniformly convergent finite element methods for singularly perturbed elliptic boundary value problems I: Reaction-diffusion type, *Computers Math. Applic.* **35** (3), 57–70, (1998).
4. R. Verfürth, Robust *a posteriori* error estimators for a singularly perturbed reaction-diffusion equation, *Numerical Mathematik* **78**, 479–493, (1996).
5. M. Ainsworth and I. Babuška, Reliable and robust *a posteriori* error estimation for singularly perturbed reaction-diffusion problems, *SIAM J. Numerical Analysis* **36** (2), 331–353, (1999).
6. R.E. Bank, J.F. Bürgler, W. Fichtner and R.K. Smith, Some upwinding techniques for finite element approximations of convection-diffusion equations, *Numer. Math.* **58**, 119–128, (1990); http://sdna3.ucsd.edu/~reb/.
7. R.E. Bank and D.J. Rose, Global approximate Newton methods, *Numer. Math.* **37**, 279–295, (1981); http://sdna3.ucsd.edu/~reb/.
8. R.E. Bank and L.R. Scott, On the conditioning of finite element equations with highly refined meshes, *SIAM J. Numerical Analysis* **26**, 1383–1394, (1989); http://sdna3.ucsd.edu/~reb/.
9. C.A. Xenophontos, The *hp* finite element method for singularly perturbed problems, Ph.D. Dissertation, University of Maryland, Baltimore, MD, (1996); http://www.clarkson.edu/~christos/PSFILES/publications.html.
10. C.A. Xenophontos, The *hp* finite element method for singularly perturbed problems in non-smooth domains, *Numerical Methods for PDE's* **15**, 63–90, (1998); http://www.clarkson.edu/~christos/PSFILES/publications.html.
11. A.H. Schatz and L.B. Wahlbin, On the finite element method for singularly perturbed reaction-diffusion problems in two and one dimensions, *Mathematics of Computation* **40** (161), 47–89, (1989).
12. N. Maden and M. Stynes, *Efficient Generation of Oriented Meshes for Solving Convection-Diffusion Problems*, Department of Mathematics, Cork, Ireland, (1996).
13. T. Apel and G. Lube, Anisotropic mesh refinement for a singularly perturbed reaction diffusion model problem, *Appl. Numer. Math.* **26**, 415–433, (1998); http://www.tu-chemnitz.de/~tap/refs.html.
14. G.I. Shishkin, Methods of contructing grid approximations for singularly perturbed boundary-value problems. Condensing grid methods, *Russ J. Numer. Anal. Math. Modelling* **7**, 537–562, (1992).
15. R.E. Bank, Hierarchical bases and the finite element method, *Acta Numerica*, 1–100, (1996); http://sdna3.ucsd.edu/~reb/.
16. R.E. Bank and R.K. Smith, Mesh smoothing using *a posteriori* error estimates, *SIAM J. Numerical Analysis* **34**, 979–997, (1997); http://sdna3.ucsd.edu/~reb/.
17. R.E. Bank and A.H. Sherman, An adaptive, multi-level method for elliptic boundary value problems, *Computing* **26**, 91–105, (1980); http://sdna3.ucsd.edu/~reb/.
18. J. Li, Finite element applications and analysis for singularly perturbed problems and shallow-water equations, Doctoral Thesis, Florida State University, (1998).
19. J. Li and I.M. Navon, Global uniformly convergent finite element methods for singularly perturbed elliptic boundary value problems: Higher-order elements, *Computer Methods in Applied Mechanics and Engineering* **171** (1/2), 1–23, (1999).
20. J. Liand and I.M. Navon, Uniformly convergent finite element methods for singularly perturbed elliptic boundary value problems II: Convection-diffusion type, *Computer Methods in Applied Mechanics and Engineering* **162** (1–4), 49–78, (1998).
21. M.C. Rivara, Mesh refinement processes based on the generalized bissection of simplices, *SIAM J. Numerical Analysis* **21**, 604–613, (1984).